

Transgenic viral expression of PH-20, IL-12, and sPD1-Fc enhances immune cell infiltration and anti-tumor efficacy of an oncolytic virus

Soon-Oh Hong,¹ Joonsung Kim,¹ Sungmin Lee,¹ Jaeil Shin,¹ Hwanjun Choi,¹ Eunjin Lee,¹ Hyesoo Kang,¹ Hyesun Lee,^{1,6} Soondong Lee,^{1,7} Naeun Yun,^{1,7} Jiwon An,^{1,7} Heonsik Choi,^{1,7} Hyeree Kim,^{2,3} Wonseok Kang,^{2,3,4} Yeup Yoon,^{2,3,5} and Sujeong Kim¹

¹Institute of BioInnovation Research, Kolon Life Science, Seoul 07793, Republic of Korea; ²Department of Health Sciences and Technology, Samsung Advanced Institute for Health Sciences and Technology, Sungkyunkwan University, Seoul 06351, Republic of Korea; ³Institute for Future Medicine, Samsung Medical Center, Seoul 06351, Republic of Korea; ⁴Department of Medicine, Samsung Medical Center, Sungkyunkwan University School of Medicine, Seoul 06351, Korea; ⁵Department of Biopharmaceutical Convergence, Sungkyunkwan University, Suwon 16419, Republic of Korea

Oncolytic viruses are of significant clinical interest due to their ability to directly infect and kill tumors and enhance the anti-tumor immune response. Previously, we developed KLS-3010, a novel oncolytic virus derived from the International Health Department-White (IHD-W) strain vaccinia virus, which has robust tumoricidal effects. In the present study, we generated a recombinant oncolytic virus, KLS-3020, by inserting three transgenes (hyaluronidase [PH-20], interleukin-12 [IL-12], and soluble programmed cell death 1 fused to the Fc domain [sPD1-Fc]) into KLS-3010 and investigated its anti-tumor efficacy and ability to induce anti-tumor immune responses in CT26.WT and B16F10 mouse tumor models. A single injection of KLS-3020 significantly decreased tumor growth. The roles of the transgenes were investigated using viruses expressing each single transgene alone and KLS-3020. PH-20 promoted virus spread and tumor immune cell infiltration, IL-12 activated and reprogrammed T cells to inflammatory phenotypes, and sPD1-Fc increased intra-tumoral populations of activated T cells. The tumor-specific systemic immune response and the abscopal tumor control elicited by KLS-3020 were demonstrated in the CT26.WT tumor model. The insertion of transgenes into KLS-3020 increased its anti-tumor efficacy, supporting further clinical investigation of KLS-3020 as a novel oncolytic immunotherapy.

INTRODUCTION

The recent success of cancer immunotherapy has led to a fundamental change in treatment of cancer. However, despite the clinical efficacy of cancer immunotherapies, these modalities are unsuccessful in many cancer types and individual patients.¹ Several types of solid cancer, such as colorectal cancer, pancreatic cancer, and prostate cancer, are unresponsive or minimally responsive to checkpoint blockade, and, even in responsive tumors such as melanoma and lung cancer, currently available immunotherapies are

only successful in a subset of patients.¹⁻⁴ Identifying the determinant of the anti-tumor immunotherapy response is the focus of many studies, and results suggest that tumoral expression of immune checkpoints (e.g., programmed death-ligand 1 [PD-L1] and programmed cell death 1 [PD-1]) and neo-antigens derived from genomic instability is correlated with a better response and prognosis.⁵ In addition, the presence of abundant and active immune cells in tumors is a factor that determines the response to immunotherapy.⁵ Therefore, to improve the response of cancer patients to immunotherapy drugs, a multi-modal approach that can target various factors is needed.

Oncolytic viruses (OVs) are an emerging immunotherapy approach used to selectively kill tumor cells via natural tumor tropism or virus engineering. OVs induce anti-tumor immune responses in the tumor microenvironment (TME) by mediating tumor-specific antigen exposure to antigen-presenting cells for acquisition of anti-tumor immunity.^{6,7} In addition, viral infection itself boosts secretion of anti-viral cytokines (e.g., interferon [IFN]) from infected cells, shifting the TME to a pro-inflammatory environment.⁸ These molecular events enhance the anti-tumor efficacy not only by localized tumor cell removal but also by the enhancement of systemic anti-tumor immunity, thereby attenuating development of distant metastases or relapse.⁸ Despite these features, several challenges preclude clinical use of OVs to treat

Received 22 March 2023; accepted 29 August 2023;
<https://doi.org/10.1016/j.omto.2023.08.013>.

⁶Present address: Pharmaceutical Bio Research Institute, Samyang holdings, Sungnam 13488, Republic of Korea

⁷Present address: Healthcare Research Institute, Kolon Advanced Research Center, Kolon Industries, Seoul 07793, Republic of Korea

Correspondence: Dr. Sujeong Kim, Institute of BioInnovation Research, Kolon Life Science, 110 Magokdong-ro, Gangseo-gu, Seoul 07793, Republic of Korea.

E-mail: sujeong@kolon.com



cancer, such as physical blockade of virus dissemination within tumors and immunosuppressive TMEs.

Although OV_s can infect tumor cells and induce their lysis by their native characteristics, virus spread is attenuated by the physical barriers between cancer cells (e.g., the extracellular matrix [ECM] and connective tissue cells), which are a major obstacle to improving the therapeutic efficacy of OV_s. Another critical obstacle is the immunosuppressive TME of solid tumors, which protects tumors from functional anti-tumor immune responses. Therefore, viral infection of tumor cells alone is not sufficient for induction of anti-tumor immune responses to eliminate tumor cells. To overcome the current limitations of the OV approach, combination treatment with other anti-tumor therapies, or genetic modifications to equip OV_s with transgenes, have been widely utilized.⁹ In our previous study, we generated a novel OV, KLS-3010, by deleting three viral genes (C11R, J2R, and K3L) from the vaccinia virus International Health Department-White (IHD-W) strain.¹⁰ In the present study, KLS-3010 was used as a viral backbone, and three transgenes were selected to overcome the current limitations of OV approaches and increase the therapeutic efficacy of KLS-3010. The therapeutic efficacy of KLS-3020, the recombinant virus containing the three transgenes, was evaluated, as were the effects of each transgene expressed singly.

First, the hyaluronidase PH-20, which degrades hyaluronic acid (HA), a major tumor ECM component, was inserted. The purpose of PH-20 expression was to enhance the spread of the oncolytic virus within tumors by degrading the excessively dense ECM of tumors, which hinders viral spread.^{11,12} Next, we inserted the cytokine interleukin (IL)-12 to activate natural killer (NK) cells and T cells and stimulate maturation of dendritic cells (DCs) to enhance anti-tumor immunity. Although non-clinical studies support the use of IL-12 as an anti-tumor therapy, clinical trials of systemic IL-12 therapy resulted in severe side effects, necessitating development of additional modifications.^{13–15} In the present study, we applied an intratumoral IL-12 delivery approach to maximize IL-12 delivery to the TME while minimizing systemic exposure. Lastly, an extracellular domain of (PD-1) fused to the Fc domain of immunoglobulin (Ig) G (sPD1-Fc) was inserted to target PD-L1. PD-L1 is a representative immune checkpoint molecule that is often expressed in tumor cells and some immune cells such as DCs and is widely targeted by immunotherapies.^{16–18} OV_s increase effector T (T_{eff}) cell infiltration to tumors, although this effect is ultimately negated by upregulation of PD-L1 expression in tumors.^{19,20} This barrier necessitates targeting of PD-L1 to enhance the anti-tumor effects of OV_s.^{21–23} sPD1-Fc functions as an interactor for PD-L1 on the surface of tumor cells and inhibits the interaction with PD-1 on the surface of immune cells to sustain T cell immunity.²⁴ Also, the Fc domain of sPD1-Fc induces antibody-dependent cell death.²⁵

In the present study, we show that inserting PH-20, IL-12, or sPD1-Fc into the KLS-3010 virus increases the anti-tumor effects of oncolytic virotherapy in tumor-bearing mouse models, and that combined expression of the three transgenes in KLS-3020 markedly

suppresses *in vivo* tumor growth. Furthermore, KLS-3020 elicited systemic tumor-specific immunity, suggesting its efficacy in inducing immune surveillance to prevent the development of metastases and relapse.

RESULTS

Construction and characterization of recombinant vaccinia viruses

In a previous study, we generated the novel oncolytic virus KLS-3010 by deletion of three viral genes (C11R, K3L, and J2R) from the vaccinia virus IHD-W strain.¹⁰ KLS-3010 has robust anti-tumor activity and activates the immune response in the tumor microenvironment. To enhance its efficacy, we developed the KLS-3020 virus by inserting human PH-20, murine IL-12, and murine sPD1-Fc into KLS-3010 (Figure 1A). Gene modifications in the desired sites were confirmed by PCR (Figure S1), and transgene expression was confirmed by western blotting to detect the expression of PH-20, IL-12, and sPD1-Fc (Figure 1B). The expression of IL-12 was quantified in a time- and dose-dependent manner using an ELISA method (Figure 1C). Recombinant vaccinia viruses (rVVs) containing each single gene were also generated (KLS-3010-PH-20, KLS-3010-IL-12, and KLS-3010-sPD1-Fc) (Figure S2).

Single injection of KLS-3020 significantly reduces tumor growth in colon and melanoma tumor models

First, we investigated whether the anti-tumor efficacy of KLS-3020 was increased by transgene insertion into KLS-3010 in the CT26.WT and B16F10 syngeneic tumor models. Because KLS-3020 is an oncolytic virus containing transgenes that activate anti-tumor immune responses, we used immune-competent models instead of immune-deficient animals such as athymic or severe combined immunodeficiency (SCID) mice. CT26.WT and B16F10 tumors were used because they are considered immunologically “hot” and “cold” tumors, respectively,²⁶ and are thus appropriate to investigate the efficacy of KLS-3020 in tumors with distinct immunological features. When the average tumor size reached about 100 mm³, PBS, KLS-3010, or KLS-3020 (1×10^7 median tissue culture infective dose (TCID₅₀) in CT26.WT tumors or 1×10^5 TCID₅₀ in B16F10 tumors) was injected intratumorally. A single injection of KLS-3020 inhibited tumor growth more effectively than KLS-3010 in both tumor models (Figure 2). In addition, KLS-3020 significantly prolonged the survival of tumor-bearing mice compared with other groups.

PH-20 in rVV augments virus spread and immune cell infiltration in tumors

To investigate the effects of each individual transgene on OV efficacy, we first tested the effect of PH-20 on the TME. Substantial ECM deposition in tumors functions as a physical barrier to suppress the spread of OV_s to adjacent tumor cells.²⁷ Mainly, the tumor ECM comprises proteins such as collagen, fibronectin, laminins, and tenascins, and proteoglycans such as HA. HA is the most overproduced ECM molecule in multiple tumor types and contributes significantly to the rigidity of the tumor ECM.²⁸ The amount of HA deposition is relatively high in glioblastoma, skin melanoma, and uterine carcinoma and

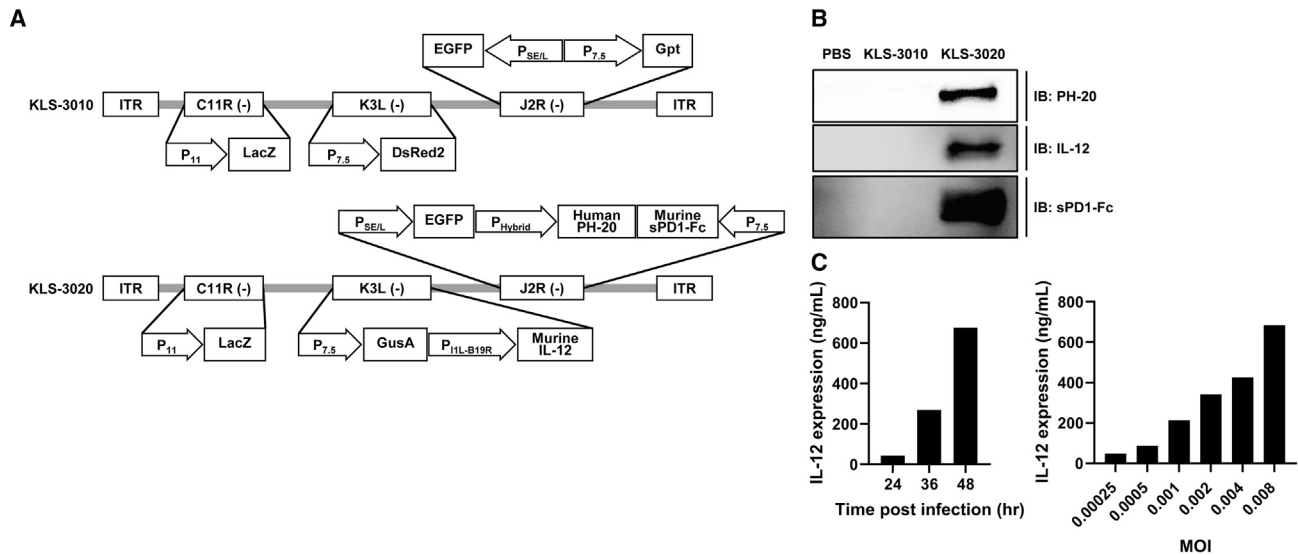


Figure 1. Construction and characterization of recombinant vaccinia viruses

(A) Schematic diagram of the genomic structure of recombinant viruses. KLS-3010 was constructed by deleting three viral genes (C11R, K3L, and J2R) from IHD-W strain vaccinia virus and three reporter genes (LacZ, eGFP, and GusA) were inserted to each locus of the deleted gene. KLS-3020 was constructed by inserting three transgenes (PH-20, IL-12, and sPD1-Fc) to KLS-3010. ITR, inverted terminal repeat; LacZ, β -galactosidase; eGFP, enhanced green fluorescent protein; Gus A, β -glucuronidase. (B) Protein expression of PH-20, IL-12, and sPD1-Fc by KLS-3020 were confirmed by western blot analysis. HeLa cells were infected with the corresponding virus at the multiplicity of infection (MOI) of 0.05 and the cultured medium was harvested after 48 h for the analysis. (C) Time- and dose-dependent expression of IL-12 by KLS-3020 was quantified by ELISA. For analysis of time-dependent expression, HeLa cells were infected with KLS-3020 at an MOI of 0.01 and the medium was harvested after 24, 36, and 48 h for the analysis (left). For analysis of dose-dependent expression, HeLa cells were infected with KLS-3020 at an MOI from 0.00025 to 0.008 and the medium was harvested after 48 h for the analysis (right).

closely associated with HA synthase 2 (HAS) expression.^{29,30} Therefore, we overexpressed PH-20, an enzyme that degrades HA, to potentially increase the therapeutic efficacy of the OV by degrading HA deposited in the tumor microenvironment.

We confirmed the enzymatic activity of PH-20 expressed by KLS-3010-PH-20 using an *in vitro* HA degradation assay. CT26.WT and B16F10 cells were treated with PBS, KLS-3010, or KLS-3010-PH-20 (multiplicity of infection [MOI] = 0.1). At 72 h after infection, the media were harvested and assessed for its ability to degrade HA. The media from cells treated with KLS-3020 showed bioactivity at 20–30 U/mL, whereas those from cells treated with PBS or KLS-3010 did not. The results suggest that PH-20 secreted from KLS-3010-PH-20-infected cells successfully degraded HA (Figure S3). Subsequently, to evaluate the effects of PH-20 on intratumoral virus spread, PBS, KLS-3010, or KLS-3010-PH-20 was injected intratumorally into CT26.WT (1×10^8 TCID₅₀) and B16F10 tumors (1×10^6 TCID₅₀) when the average tumor size reached about 100 mm³. Three days after virus injection, tumors were harvested and viral spread was compared. As KLS-3010 and KLS-3010-PH-20 contain an enhanced green fluorescence protein (EGFP) gene as a reporter, the fluorescent area within the tumor was measured. The results showed that the EGFP+ area was significantly enlarged by PH-20 expression in both tumor-bearing mouse models, suggesting that HA degradation increases the spread of the OV (Figure 3A).

Based on a previous study suggesting that degradation of the tumoral ECM increases immune cell infiltration,³¹ we examined whether immune cell infiltration in the tumor was enhanced by KLS-3010-PH-20. PBS, KLS-3010, or KLS-3010-PH-20 was injected intratumorally into CT26.WT tumors at a dose of 1×10^8 TCID₅₀, and tumors were harvested 5 days later for analysis of intratumoral immune cell populations. Injection of KLS-3010 or KLS-3010-PH-20 increased intratumoral infiltration of CD4⁺ T cells and CD8⁺ T cells compared with PBS, and the intratumoral immune cell population was further increased by KLS-3010-PH-20 (Figure 3B). Considering the total population of CD4⁺ and CD8⁺ T cells, PH-20 expression significantly increased the infiltration of immune cells. These findings suggest that degradation of HA by expression of PH-20 in KLS-3010-PH-20 increases virus transmission and immune cell infiltration in tumors.

IL-12 in rVV increases T cell activation and differentiation

IL-12 is a pro-inflammatory cytokine that regulates the T cell and NK cell responses, induces production of interferon-gamma (IFN- γ) by CD4⁺ T, CD8⁺ T, and NK T cells, and increases differentiation of type I helper T (T_{H1}) cells. Therefore, we investigated the effect of KLS-3010-IL-12 on T cell activation and differentiation in CT26.WT and B16F10 tumor-bearing mice. After induction of tumor formation, KLS-3010 or KLS-3010-IL-12 was injected into CT26.WT tumors (1×10^7 TCID₅₀) and B16F10 tumors (1×10^5 TCID₅₀). PBS was injected as a negative control. Five days following injection,

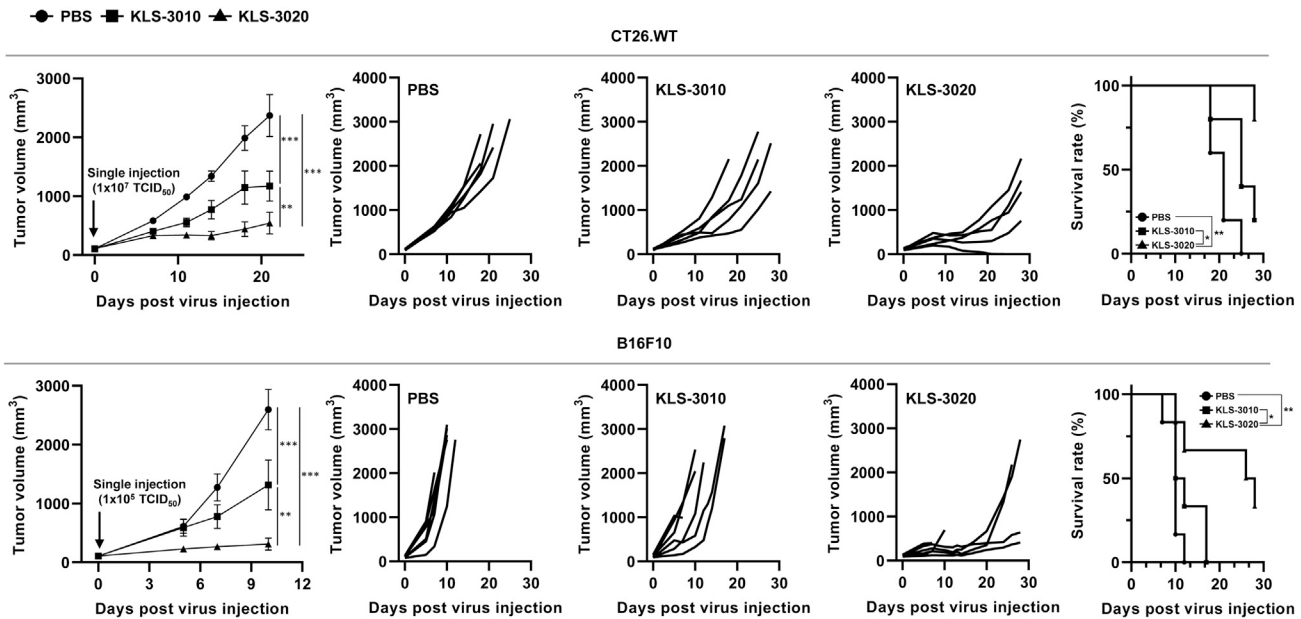


Figure 2. *In vivo* anti-tumor efficacy of KLS-3020 in CT26.WT and B16F10 tumor-bearing mouse models

The *in vivo* anti-tumor effects of KLS-3020 were evaluated in various syngeneic mouse tumor models. CT26.WT (colon cancer) cells were subcutaneously injected to BALB/c mice and B16F10 (melanoma) cells were subcutaneously injected to C57BL/6 mice. PBS or virus was intratumorally injected when average tumor volume reached about 100 mm³. As a humane endpoint, the mouse was sacrificed when the individual tumor volume reached 2,000 mm³. The average tumor volume (left), the individual tumor volume (middle), and the survival rates (right) of PBS-, KLS-3010-, or KLS-3020-treated group are depicted. Data are expressed as the mean \pm SEM. **p* < 0.05, ***p* < 0.01, ****p* < 0.001.

tumors were excised and intratumoral immune cell populations were analyzed. The ratios of CD8⁺IFN- γ ⁺ cells within the total CD8⁺ T cell population, and CD4⁺IFN- γ ⁺ cells within the total CD4⁺ T cell population, were increased by KLS-3010 and KLS-3010-IL-12 when compared with PBS (Figure 4A). Total tumoral populations of activated T_{eff} cells, such as CD4⁺IFN- γ ⁺ and CD8⁺IFN- γ ⁺, in both tumor models were increased to a greater extent by KLS-3010-IL-12 than by KLS-3010, supporting the immune-activating roles of IL-12 expression in rVVs (Figure S4). To precisely investigate the role of IL-12 in helper T cell differentiation, we also assessed the population of T_{h2} (CD4⁺IL-4⁺) cells relative to the T_{h1} (CD4⁺IFN- γ ⁺) cell population. Differentiation into the T_{h1} phenotype was increased by KLS-3010, and further increased by KLS-3010-IL-12 (Figure 4A), while differentiation into the T_{h2} cell phenotype was not changed by administration of either recombinant virus (Figure 4B). These changes elicited by KLS-3010-IL-12 increased the T_{h1}/T_{h2} ratio in the tumor-infiltrating CD4⁺ T cell population by >2-fold, although the changes were not statistically significant because of in-group variation. Taken together, these findings indicate that arming KLS-3010 with IL-12 significantly increases T cell activation and induces differentiation to the T_{h1} phenotype in the TME.

sPD1-Fc in rVV sustains the active T cells

OVs eradicate tumors not only directly by infecting tumor cells and inducing cell lysis but also by controlling tumor growth via activation of tumor-specific T cell responses. However, expression of the

immune checkpoint molecule PD-L1 in tumor cells and immune cells such as DCs and tumor-associated macrophages (TAMs) decreases anti-tumor immunogenicity by binding to PD-1 on the T cell surface and inducing T cell exhaustion.^{19,20,32,33} To overcome PD-L1-mediated immunosuppression and to enhance the efficacy of KLS-3010, the sPD1-Fc transgene was inserted into KLS-3010. To determine the effects of KLS-3010-sPD1-Fc on sustaining the activity of T cells, we analyzed the activation status of tumor-residing T cells after intratumoral injection of PBS, KLS-3010, or KLS-3010-sPD1-Fc (CT26.WT tumors 1×10^8 TCID₅₀; B16F10 tumors 1×10^6 TCID₅₀). Five days after injection, tumors were excised and intratumoral immune cell populations were analyzed. T_{h1} (CD4⁺IFN- γ ⁺) cells and active T_c (CD8⁺IFN- γ ⁺) cells were increased by KLS-3010 and increased further by KLS-3010-sPD1-Fc in both models, indicating a significant increase of T_{eff} cells caused by sPD1-Fc (Figure 5A). Subsequently, we analyzed the tumoral T_{eff}/regulatory T (T_{reg}) ratio to determine the population of active immune cells relative to that of suppressive immune cells. T_{reg} (CD4⁺CD25⁺FoxP3⁺) cells are major suppressors of IFN- γ secretion from CD4⁺ T cells and CD8⁺ T cells, which diminishes active T cell numbers and facilitates tumor immune escape.³⁴ KLS-3010 and KLS-3010-sPD1-Fc did not affect the population of T_{reg} cells in CT26.WT tumors but increased the T_{reg} cell population in B16F10 tumors (Figure 5B). However, KLS-3010-sPD1-Fc increased the T_{eff}/T_{reg} ratio compared with the effect of KLS-3010 in both models, although this reached statistical significance only in

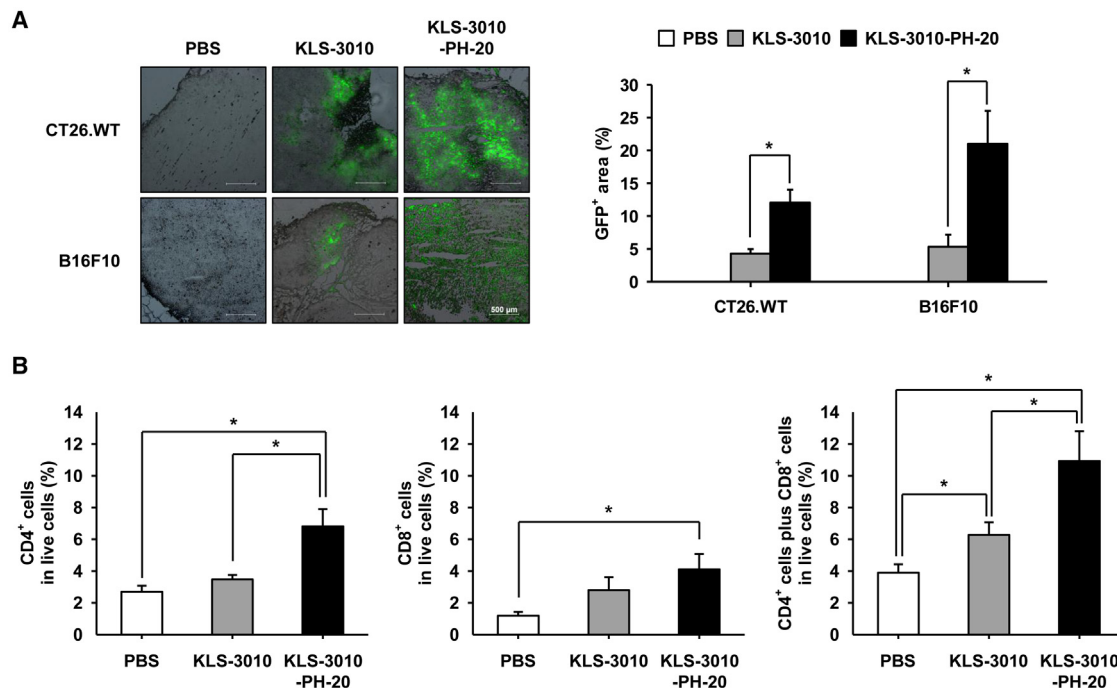


Figure 3. Expression of PH-20 by rVV enhances viral spread and immune cell infiltration

To investigate the viral spread and immune cell infiltration by PH-20 transgene expression, PBS, KLS-3010, or KLS-3010-PH-20 was intratumorally injected to mice bearing CT26.WT (1×10^8 TCID₅₀) or B16F10 (1×10^6 TCID₅₀) tumor. (A) After 3 days from virus injection, the spread of the oncolytic virus was assessed by the distribution of eGFP by confocal microscopy. Scale bar, 500 μ m. The fluorescent area was quantified based on three different pictures from each mouse ($n = 3$, total nine pictures). (B) After 5 days from virus injection, the CT26.WT tumor was harvested and the populations of tumor-infiltrating CD4⁺ T cell, CD8⁺ T cells, and total CD4⁺ T cells and CD8⁺ T cells were assessed by flow cytometry ($n = 6$). Data are expressed as the mean \pm SEM. * $p < 0.05$.

CT26.WT tumors (Figure 5C). As the proportion of total T_{reg} cells in the B16F10 model was markedly lower than that in the CT26.WT model (5.91% in CT26.WT vs. 0.25% in B16F10 of each PBS group), the significant increase in the number of total T_{eff} cells could be more important than the subtle changes in the number of total T_{reg} cells in the B16F10 tumor model with respect to generation of anti-tumor immunity by KLS-3010-sPD1-Fc. The results suggest that sPD1-Fc expression sustains T cell activity, thereby increasing the population of active T cells in the TME by inhibiting the interaction between immune checkpoint molecules.

KLS-3020 strengthens the immune response in tumors

The results showing that the expression of each individual transgene augmented the immune response in tumors prompted us to investigate whether KLS-3020 containing all three transgenes had the same effects. When the average tumor size reached about 100 mm³, PBS vehicle control, KLS-3010, or KLS-3020 was injected intratumorally (CT26.WT 1×10^7 TCID₅₀; B16F0 1×10^5 TCID₅₀). Combined expression of the three transgenes would be expected to induce a considerably greater immune response and, therefore, the injection dose of KLS-3020 was determined to be 10-fold lower than that of KLS-3010 with each transgene. Five days after injection, tumors were excised for measurement of intratumoral immune cell infiltration, activation, and differentiation. Compared with KLS-3010,

KLS-3020 significantly enhanced intratumoral infiltration of CD4⁺ T cells in the CT26.WT model and CD8⁺ T cells in the B16F10 model (Figure 6A). The total number of tumor-infiltrating CD4⁺ T cells and CD8⁺ T cells in both models was increased markedly by KLS-3020 compared with that in the PBS group or the KLS-3010 group. The active subpopulation of infiltrating CD4⁺ and CD8⁺ T cells was also increased by KLS-3020 compared with PBS or KLS-3010 (Figure 6B), which led to the increased number of active T_c cells in both models and T_{h1} cells in the CT26.WT model (Figure S5). Regarding helper T cell differentiation, KLS-3020 increased the T_{h1} cell population by >1.5-fold compared with KLS-3010 in both models, but had no effect on the T_{h2} cell population (Figure 6B). Activation and differentiation of T cells increased T_{eff} cell populations and the T_{eff}/T_{reg} ratio in tumors injected with KLS-3020 relative to tumors injected with KLS-3010 (Figure 6C). Although KLS-3020 increased the number of T_{reg} cells in the CT26.WT model significantly, the T_{eff}/T_{reg} ratio in both models was increased consistently by KLS-3020 relative to KLS-3010. The pattern of changes in T cell activation and differentiation were consistent with those induced by single expression of IL-12 or sPD1-Fc (Figures 4 and 5). The results also showed that changes, including immune infiltration and T_{eff} population, occurred at a comparable level in response to a 10-fold higher dose of KLS-3010-PH-20 or -sPD1-Fc. In addition, T helper type I differentiation and cytotoxic T cell activation were further increased by the same dose of

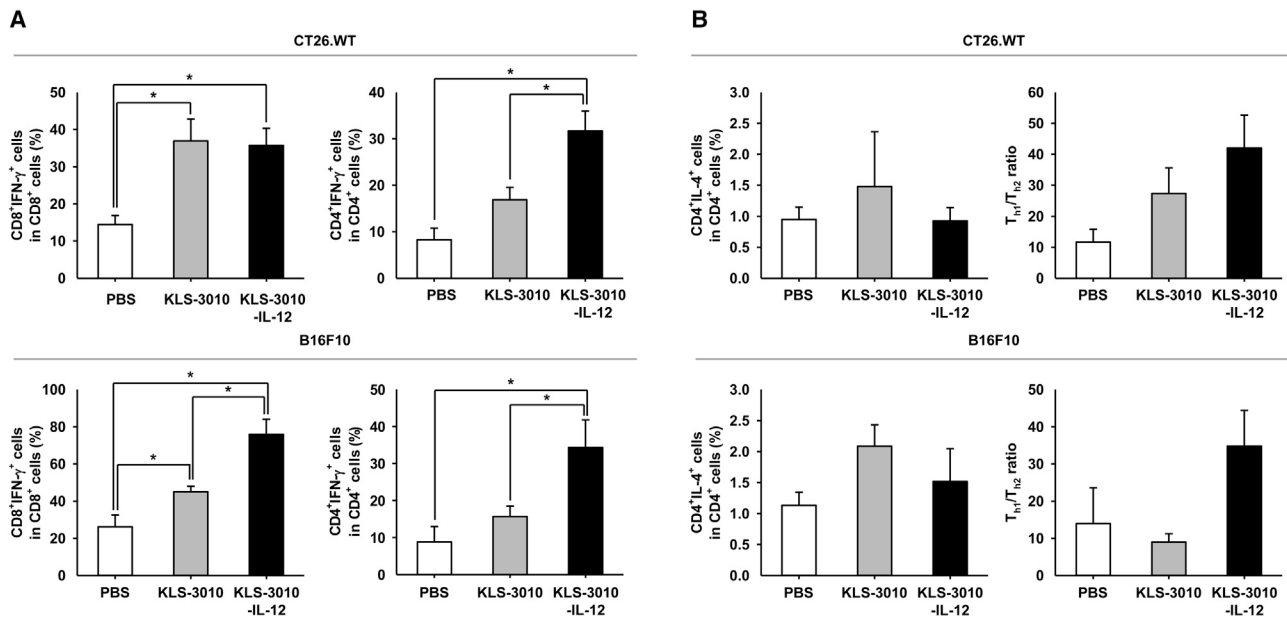


Figure 4. Expression of IL-12 by rVV increases T cell activation and differentiation

To investigate the T cell activation and differentiation by IL-12 transgene expression, PBS, KLS-3010, or KLS-3010-IL-12 was intratumorally injected to mice bearing CT26.WT (1×10^7 TCID₅₀) or B16F10 (1×10^5 TCID₅₀) tumor when the average volume reached about 100 mm³ (n = 5). (A) The populations of activated cytotoxic T (T_C) cells in CD8⁺ T cells and type I helper T (T_{H1}) cells in CD4⁺ T cells in tumor were assessed by flow cytometry. (B) The population of type II helper T (T_{H2}) cells in CD4⁺ T cells in tumor was assessed by flow cytometry and the ratio of T_{H1}/T_{H2} was calculated. Data are expressed as the mean \pm SEM. *p < 0.05.

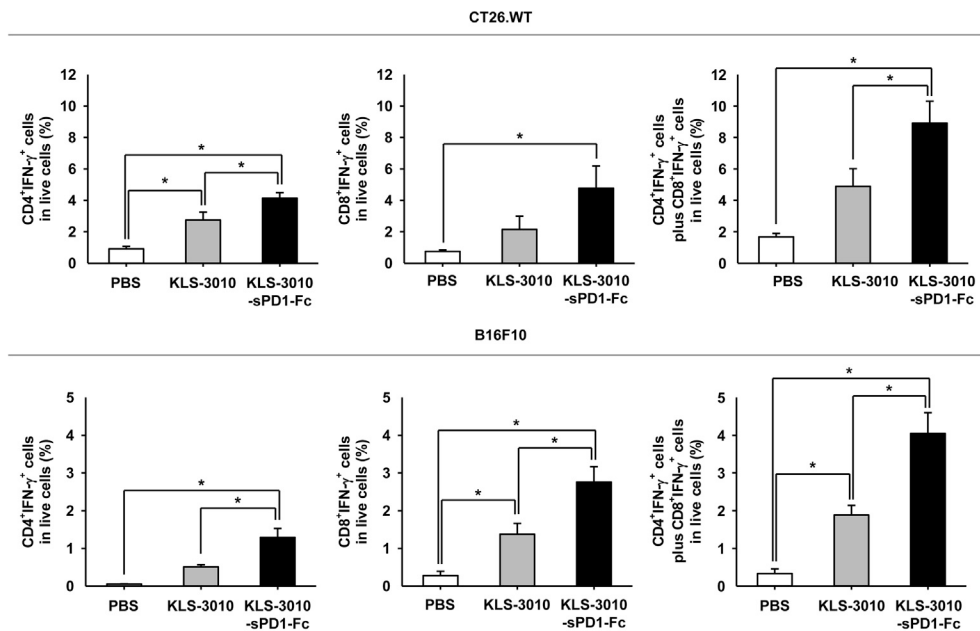
KLS-3010-IL-12. Taken together, these data demonstrate that combined expression of the three transgenes has interactive effects that strengthen the immune response induced by each transgene in the TME.

KLS-3020 induces systemic anti-tumor immune activation

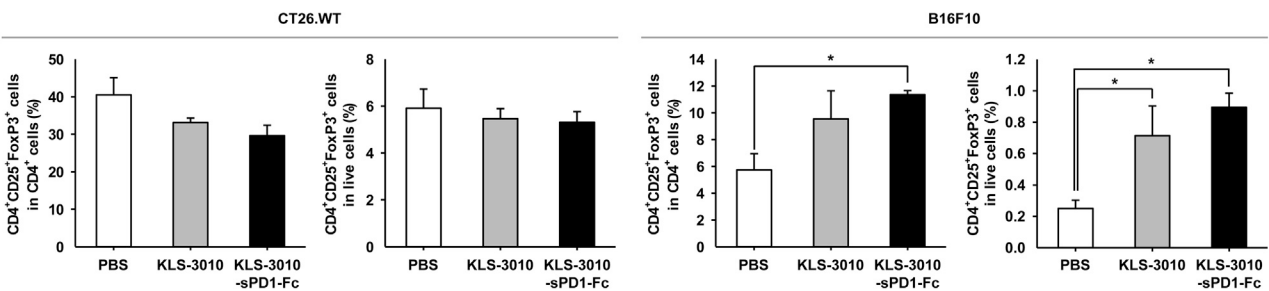
For improved tumor control and inhibition of tumor relapse, the systemic anti-tumor immune response must be activated. Therefore, we investigated whether KLS-3020 induced a systemic cancer-specific immune response in tumor-bearing mice. Because the development of adaptive immunity requires several days to a few weeks and B16F10 tumors were more likely eliminated by single injection of KLS-3020 within a short time (Figure 2, lower panel), we hypothesized that the duration of tumor-associated antigen (TAA) presentation to immune cells was shorter in B16F10 tumors than in CT26.WT tumors. Therefore, we selected CT26.WT tumor-bearing mice for the study. To maximize the immune response induced by the OV, we performed multiple injections of KLS-3020 following previously published protocols.^{35,36} PBS or KLS-3020 (8×10^7 TCID₅₀; three injections at 2-day intervals) was intratumorally injected into CT26.WT tumors when the average tumor size reached about 100 mm³. Twenty-eight days after the first injection, we excised the spleen, exposed splenocytes to CT26.WT cells, and assessed the number of IFN- γ -positive splenocytes. The enzyme-linked immunospot (ELISPOT) assay showed that splenocytes from mice treated with KLS-3020 formed a greater number of spots consisting of IFN- γ -positive splenocytes after stimulation with

CT26.WT cells than splenocytes from mice treated with PBS (p = 0.052; Figure 7A). Although the spot count changes were not statistically significant, the marked increase indicated induction of a tumor-specific immune response in immune cells distant from the tumor mass. To assess the ability of KLS-3020 to induce a systemic immune response against tumors, we investigated whether KLS-3020 could control tumors not treated with KLS-3020, as well as those treated with KLS-3020. For this purpose, we established a bilateral syngeneic mouse tumor model by implanting CT26.WT tumor cells into the right and left flanks of BALB/c mice. We implanted 5×10^5 cells in the right flank as a test article-injection tumor and 5×10^4 cells into the left flank as a non-injection tumor. Several days are required after exposure to TAA to induce a systemic immune response; during this time, the tumor mouse model should not reach the humane endpoint (i.e., the sum of the two tumor volumes of mice in all groups should be <2,000 mm³). To satisfy these conditions, we used a bilateral tumor model in which different numbers of tumor cells are injected into each side.^{37–39} Subsequently, we injected KLS-3020 only into the right flank tumor (1×10^7 TCID₅₀; three injections at 2-day intervals). Eighteen days after the first injection, tumors injected with KLS-3020 almost completely regressed, and the size of the untreated distal tumor did not increase significantly (Figure 7B). In summary, KLS-3020, an OV expressing PH-20, IL-12, and sPD1-Fc, demonstrated significant potential as anti-cancer therapy due to successful enhancement of both oncolytic activity and systemic anti-tumor immune responses in comparison to the parent virus without transgene expression.

A



B



C

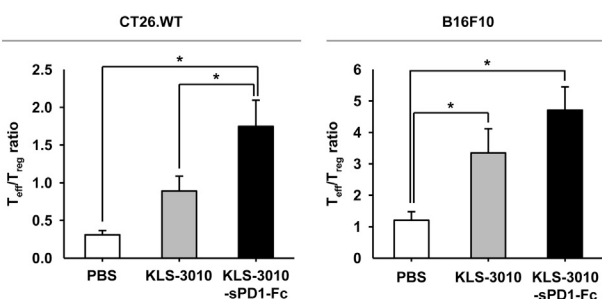


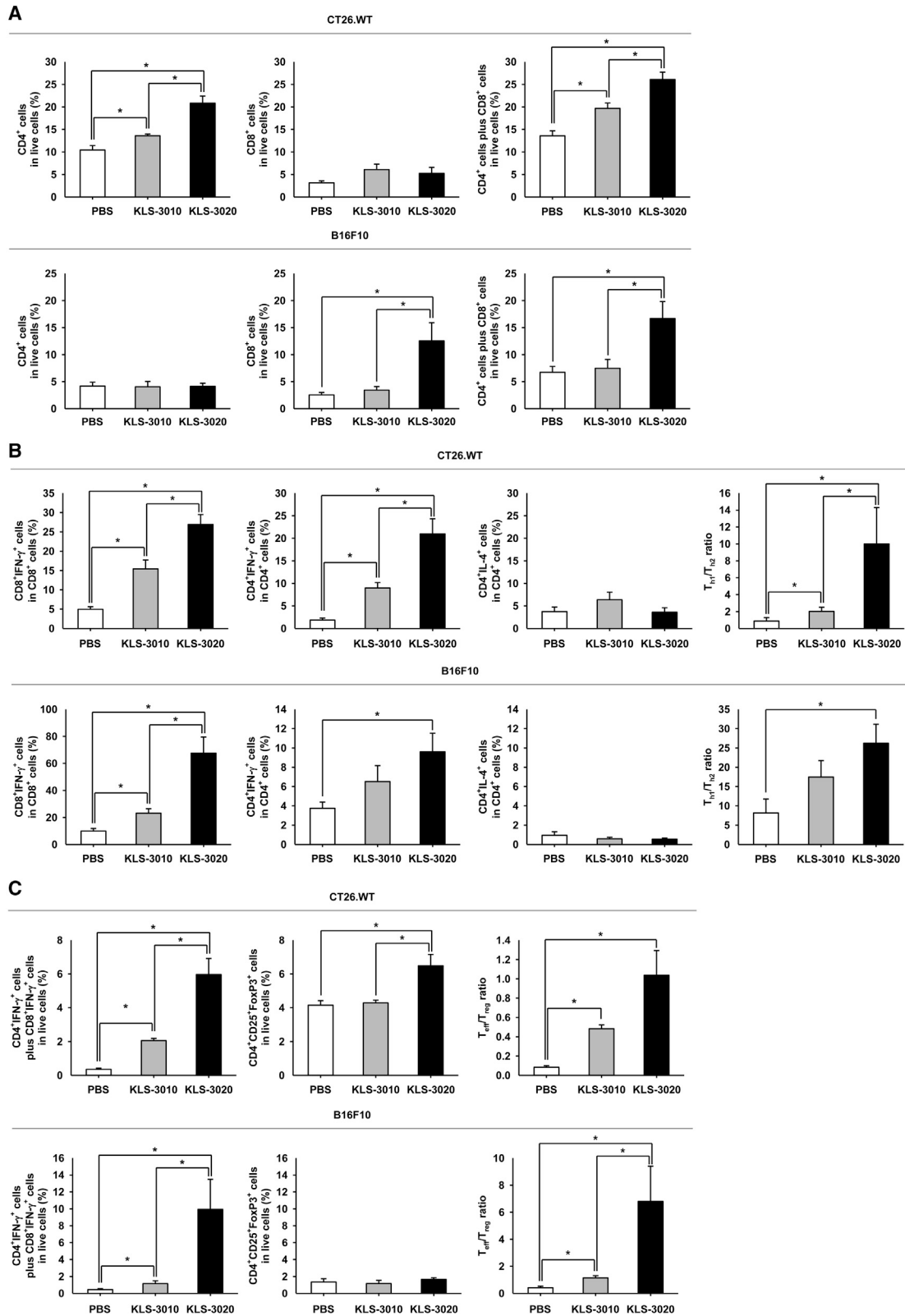
Figure 5. Expression of sPD1-Fc by rWV sustains activated T cells in tumor

The maintenance of T cell activation by sPD1-Fc expression was measured following the intratumoral injection of PBS, KLS-3010, or KLS-3010-sPD1-Fc to mice bearing CT26.WT (1×10^8 TCID₅₀) or B16F10 (1×10^6 TCID₅₀) tumor (n = 5). (A) The population of activated T_C cells and T_{H1} cells in tumor were assessed by flow cytometry. Then T_{eff} cells in tumor were calculated. (B) The population of regulatory T (T_{reg}) cells in CD4⁺ cells or in tumor was assessed by flow cytometry. (C) The T_{eff}/T_{reg} ratio was calculated. Data are expressed as the mean \pm SEM. *p < 0.05.

DISCUSSION

Cancer immunotherapy is an intensely investigated therapeutic modality that is highly effective in multiple tumor types, e.g., lung and skin cancers. However, cancer cells utilize multiple strategies to evade and suppress anti-cancer immune responses, such as prevention of

immune cell recruitment, expression of immune checkpoint molecules, and immunosuppressive differentiation.^{40,41} Therefore, immunotherapies are only effective in a subset of tumor types lacking these capabilities. Development of improved immunotherapies to bypass these defenses will address a significant unmet clinical need.



(legend on next page)

OVs are emerging as promising anti-tumor agents that reverse tumor-mediated immunosuppression via unique mechanisms. In addition to selective tumor lysis, OVs induce changes in the TME by activating both the innate and adaptive immune responses.⁴² Similar to other immunotherapies, the efficacy of OVs is closely related to the status of the TME, and most components in the TME inhibit the efficacy of OVs. Suppression of OV spread by barriers such as a dense ECM deposited in tumors is a significant limiting factor that reduces viral transmission following intratumoral injection.^{43,44} Furthermore, mechanisms of immunosuppression in the TME, such as expression of immune checkpoints on various cells, can restrict OV-mediated activation of antitumoral immunity.²⁰

In the present study, we generated KLS-3020, a novel oncolytic virus engineered with three transgenes to maximize the therapeutic efficacy of virotherapy. The ECM occupies the extracellular region in the TME and the rigid structure of the unusually dense ECM functions as a physical barrier to inhibit viral spread to initially uninfected tumor cells. The impenetrability of the TME ECM can be also an obstacle to immune cell infiltration.^{45–47} Although ECM profiles differ between tumor types, HA is a major ECM component secreted by cancer-associated fibroblasts in the TME.²⁸ To overcome the ECM-related limitations of OVs, we introduced PH-20 into the KLS-3010 to degrade HA in the TME. PH-20 significantly increased infection of tumor cells by the virus as well as subsequent tumoral infiltration of T cells (Figure 3). Prior studies investigating the effects of ECM degradation by OVs demonstrated the additive advantages of this process. Degradation of the ECM was related to the increase of oncolysis, *in vivo* efficacy, and the upregulated expression of transgenes encoded by OVs via increased viral replication and infection.^{43,44,48} These findings support the significant role of PH-20 in increasing the effects of the transgenes inserted into KLS-3020.

IL-12 is a potent pro-inflammatory type 1 cytokine that has long been studied as a potential cancer immunotherapy agent. The significant effects of IL-12 on immune activation, and the subsequent anti-tumor effects mediated by IFN- γ expression in T and NK cells, are well accepted.¹³ IL-12 was a successful anti-tumor agent in preclinical studies.¹³ These findings prompted multiple clinical studies in the mid-1990s, in which IL-12 was administered as a systemic cytokine therapy, but these trials failed due to severe unmanageable toxicity.⁴⁹ As an alternative approach, localized expression of IL-12 via gene or gene-modified cell therapy has considerable therapeutic efficacy with reduced toxicity, although there are no approved products to date.^{50,51} Local delivery of IL-12 facilitates CD8⁺ T cell infiltration into tumors and activates the antigen presentation machinery, resulting in expansion of tumor-specific CD8⁺ effector T cells.⁴⁹ In the pre-

sent study, intratumoral injection of OV induced the expression of IL-12 primarily in the injected tumor, maintaining the spatiotemporal distribution of IL-12 in the tumor, and leading to the local delivery. We demonstrate that local intratumoral injection of KLS-3010-IL-12 and KLS-3020 increases the number of T_{eff} cells (CD4⁺IFN- γ ⁺ and CD8⁺ IFN- γ ⁺), which can enhance the *in vivo* efficacy (Figures 4 and 6), and there were no severe adverse events in the treated mice (data not shown). Taken together, these findings suggest that OVs harboring IL-12 as a transgene are an alternative delivery approach for IL-12 to the TME.

Expression of immune checkpoint molecules on the surface of tumor cells is a major determinant of immunotherapy efficacy.⁵² The PD-1/PD-L1 and -L2 pathway is a representative of negative immunoregulatory signaling that facilitates the immune evasion of cancer cells.²⁰ PD-1 is most commonly expressed on activated lymphocytes such as CD4⁺ T and CD8⁺ T cells, NK T cells, B cells, and activated monocytes and is bound with its ligand, PD-L1.^{53,54} PD-L1 is expressed in diverse tumor cell types, including melanoma and lung, colorectal, and breast cancers.^{54–57} Interaction of PD-1 with PD-L1 inhibits the activity of effector T cells, especially tumor-infiltrating lymphocytes (TILs), while simultaneously enhancing the function and development of immunosuppressive T_{reg} cells, ultimately allowing tumor cells to evade the immune response.⁵⁸ Therefore, blockade of PD-1/PD-L1 augments anti-tumor immunity by restoring the activity of effector T cells and decreasing the number and/or suppressive activity of T_{reg} cells.⁵⁸ Hypoxia, which is a common characteristic of the TME, boosts the expression of PD-L1 at the transcriptional level by hypoxia-inducible factor 1 alpha (HIF-1 α).⁵⁹ In addition, the IFN- γ signaling pathway, which is activated by OV infection, increases PD-L1 expression by tumor cells.²¹ These studies highlight the need to control PD-L1 activity to improve OV therapies. Therefore, we inserted soluble PD-1 in KLS-3020 to block the PD-1/PD-L1 axis. In the present study, we confirmed that regional expression of sPD1-Fc via our engineered vaccinia virus increased the population of activated T cells in tumors compared with KLS-3010 (Figure 5). These findings demonstrate that an oncolytic vaccinia virus engineered to express a PD-L1 modulator has the potential to improve the therapeutic efficacy of immunotherapies. Although Fc-mediated antibody effector functions were not investigated in the present study, the Fc domain of sPD1-Fc is expected to induce antibody-dependent cancer cell death, thereby contributing to the therapeutic efficacy of KLS-3020.

Simultaneous expression of the three transgenes by KLS-3020 significantly increased immune cell infiltration and the populations of activated effector T cells in KLS-3020-injected tumors relative to tumors injected with KLS-3010 (Figure 6). Increased TILs likely upregulate

Figure 6. Enhanced anti-tumor immune response by KLS-3020

The changes of immune response by the combinatorial expression of three transgenes in KLS-3020 were investigated. PBS, KLS-3010, or KLS-3020 was intratumorally injected to mice bearing CT26.WT (1×10^7 TCID₅₀) or B16F10 (1×10^5 TCID₅₀) tumor (n = 6). (A) The populations of CD4⁺ T cells, CD8⁺ T cells, and total CD4⁺ T and CD8⁺ T cells in tumor were assessed by flow cytometry. (B) The populations of activated T_c cells in CD8⁺ T cells, T_{h1} cells in CD4⁺ T cells, and T_{h2} cells in CD4⁺ T cells in tumor were assessed by flow cytometry and the ratio of T_{h1}/T_{h2} was calculated. (C) The populations of T_{eff} cells and T_{reg} cells in tumor were assessed by flow cytometry and the ratio of T_{eff}/T_{reg} was calculated. Data are expressed as the mean \pm SEM. *p < 0.05.

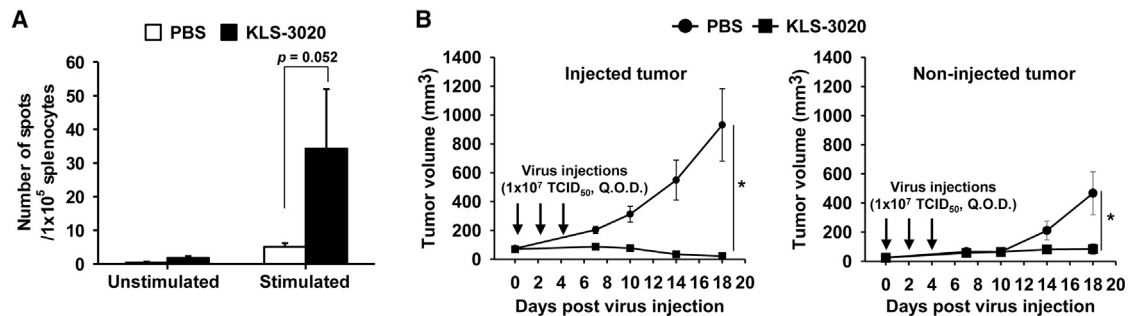


Figure 7. Systemic anti-tumor immune activation by KLS-3020

Systemic and cancer-specific immune response was induced by KLS-3020. (A) The acquisition of cancer-specific immune response was assessed by ELISPOT assay measuring IFN- γ secreting splenocytes. PBS or KLS-3020 (8×10^7 TCID₅₀) was intratumorally injected three times every other day to mice bearing CT26.WT tumor ($n = 6$). After 28 days from first virus injection, splenocytes were harvested, incubated with CT26.WT for stimulation, and stained to measure the activation. (B) To investigate the occurrence of systemic immune response by KLS-3020, CT26.WT cells were implanted into right flank (5×10^5 cells) and left flank (5×10^4 cells) of BALB/c mice. After 7 days, PBS or KLS-3020 (1×10^7 TCID₅₀) was intratumorally injected three times every other day to only tumor on right flank. The tumor volume was measured until that of the KLS-3020 group was diagnosed as complete regression. Data are expressed as the mean \pm SEM. * $p < 0.05$.

secretion of inflammatory cytokines and chemokines, further promoting recruitment of immune cells into tumors, thereby improving anti-tumor efficacy. We postulate that this is an important regulatory mechanism for robust inhibition of tumor growth in mouse tumor models treated with KLS-3020 (Figure 2).

As shown in Figure 6, the CT26.WT and B16F10 tumor models showed differences in basal immune profiles such as T cell infiltration and T_{eff} cell populations, supporting that the CT26.WT and B16F10 models are immunologically hot and cold, respectively.²⁶ In addition, the patterns of changes in subpopulations of T cells such as CD4⁺ T, CD8⁺ T, T_{H1}, and T_{reg} cells after KLS-3020 treatment were not identical between the two models (Figures 6 and S5). For instance, the population of CD4⁺ T cells was not increased by administration of KLS-3020 in B16F10 tumors, whereas the population of CD8⁺ T cells was significantly augmented. In CT26.WT tumors, the population of CD4⁺ T cells was considerably increased by administration of KLS-3020 in B16F10 tumors, but the population of CD8⁺ T cells was not increased. Although the reasons for the differences between the models are not fully understood, they may be related to both the tumor type and the genetic background of the mouse strains. The cellular immune response is more developed in C57BL/6 mice, whereas the humoral immune response is more developed in the BALB/c strain.⁶⁰ Nevertheless, KLS-3020 exhibited strong immune activating effects on both tumors, resulting in significant tumor growth control (Figures 2 and 6). Multiple studies demonstrate that the B16F10 tumor model is weakly immunogenic and highly aggressive,^{61,62} showing little therapeutic response to either anti-cytotoxic T lymphocyte-associated protein 4 (CTLA-4) or -PD-L1 antibody therapies (opposite to CT26.WT).²⁶ We attribute the anti-tumor efficacy of KLS-3020 in the B16F10 tumor model to a transformation of a cold tumor type to a hot tumor type and, therefore, the effects of KLS-3020 are paramount to the success of immune checkpoint inhibitors, including anti-PD-L1, CTLA-4, LAG-3, and TIGIT antibodies.^{23,35,36,63} The present findings demonstrate that KLS-3020

has the potential to disrupt and transform the TME, overcoming resistance mechanisms of the TME for improved therapeutic efficacy.

Treatment with local radiation and systemic immunotherapy, such as immune checkpoint-blocking antibodies, has abscopal anti-tumor effects that strongly contribute to the systemic tumor control.^{64,65} Recent studies demonstrate that intratumoral OV therapy also has abscopal therapeutic effects leading to impaired growth of distant tumors not directly infected by the virus.^{36,66} The rationale for OV-mediated abscopal effects is that oncolytic replication induces immunogenic cell death and immunological danger signaling, facilitating induction of *de novo* immunity, especially that of T cells.⁶⁶ In the present study, we assessed the systemic effects of local treatment with KLS-3020 in a bilateral CT26.WT mouse tumor model. Tumors injected with KLS-3020 almost completely resolved, and growth of untreated distal non-injected tumors was minimal (Figure 7B), suggesting that OV therapy has both local and systemic tumor control effects. We did not analyze the presence of OV in distal non-injected tumors, so we cannot completely exclude the possibility that the anti-tumor response in contralateral tumors was due to direct systemic delivery of KLS-3020. However, we demonstrated that the cancer-specific immune response was induced in mice treated with KLS-3020 (Figure 7A), suggesting that KLS-3020 can systemically induce anti-tumor responses by promoting infiltration of cancer-specific T cells into the tumor. Taken together, these findings suggest that local injection of KLS-3020 can induce systemic antitumoral immune responses, supporting its potential to control distant metastases.

Taken together, we developed a novel oncolytic virus, KLS-3020, by inserting three transgenes, PH-20, IL-12, and sPD1-Fc, to improve the efficacy of the oncolytic vaccinia virus. The ability of KLS-3020 to promote recruitment of TILs, reprogram the immunosuppressive TME, and boost systemic anti-tumor immunity demonstrates that KLS-3020 is a promising potential anti-tumor immunotherapy for multiple types of solid tumors. In future studies, we plan to confirm

the safety of KLS-3020 through preclinical toxicity and bio-distribution investigations, which is critical for its clinical application.

MATERIALS AND METHODS

Cell line

HeLa (CCL-2, ATCC, Manassas, VA, USA) cells were maintained in minimum essential medium (MEM; 11090081, Gibco, Waltham, MA, USA) supplemented to contain 5% or 10% fetal bovine serum (FBS; SH30084.03, Hyclone, PA, USA), 1× antibiotic antimycotic (AA) solution (15240062, Gibco), and 2 mM L-glutamine (25030081, Gibco). CT26.WT (CRL-2638, ATCC) cells were maintained in Roswell Park Memorial Institute medium (RPMI; 11090081, Gibco) supplemented to contain 10% FBS, AA, and L-glutamine. B16F10 (CRL-6475, ATCC) and Vero (VERO01WCB-1201, MFDS, Cheongju, Korea) cells were maintained in Dulbecco's modified Eagle's medium (DMEM; LM001-08, Wellgene, Gyeongsan, Korea) supplemented to contain 10% FBS, AA, and L-glutamine. All the cells were cultured at 37°C with 5% CO₂. Before infection with the oncolytic vaccinia virus, the medium was changed from 10% to 2% FBS.

Plasmids

K3L and J2R shuttle plasmids were described in the previous report.¹⁰ Briefly, K3L shuttle plasmid 1 contains the left and right flanking regions of the K3L gene on each side of the dsRedII gene under the regulation of the p7.5 promoter, and K3L shuttle plasmid 2 contains the GusA gene instead of dsRedII. Similar to K3L shuttle plasmids, the J2R shuttle plasmid carries an EGFP gene regulated by a synthetic early/late (pE/L) promoter and left and right flanking regions of the J2R gene. About 1 kb of the flanking regions were inserted in K3L and J2R plasmids for homologous recombination with the vaccinia virus genome. Human PH-20 and murine sPD1-Fc cDNA controlled by the respective pHyb and p7.5 promoter were inserted in the J2R shuttle plasmid. Murine IL-12 cDNA was inserted into the K3L shuttle plasmid under the control of the p11L-B19R early/late promoter, which was synthesized by combining intact vaccinia promoters for *I1L* and *B19R*. The structure of shuttle plasmids was confirmed by restriction enzyme mapping and sequencing.

Recombinant vaccinia viruses

Recombinant vaccinia viruses were generated as previously described.¹⁰ KLS-3010 was used as a backbone virus to generate KLS-3010-sPD1-Fc, KLS-3010-PH-20, KLS-3010-IL-12, and KLS-3020. Briefly, HeLa cells were infected with KLS-3010 at an MOI of 0.05 TCID₅₀ and transfected with each shuttle plasmids at 15 min post infection. Then, the cells were incubated for 4 h and the medium was changed to a 5% FBS-containing medium. After incubation for 48 h at 37°C with 5% CO₂, cells were harvested, and viruses were obtained from the supernatant after three cycles of freezing and thawing. The recombinant vaccinia viruses were selected through several rounds of plaque isolation. To confirm the structure of recombinant vaccinia viruses, viral gDNA was extracted by Maxwell Viral Total Nucleic Acid Purification Kit (AS1330, Promega, Madison, WI, USA). PCR of each locus proceeded with PrimeSTAR Max DNA Polymerase (R045, Takara, Shiga, Japan) with primer sets targeting each

locus's arm region. The PCR product was electrophoresed and compared with the result of cognate shuttle plasmids.

For *in vivo* experiments, recombinant vaccinia viruses were purified by ultracentrifugation. HeLa cells were infected with the recombinant viruses. At 48 to 72 h after infection, the cells were detached by scraping and centrifuged at 1,500 rpm for 10 min at 4°C. After removing the supernatant, cells were completely resuspended with resuspension buffer (10 mM Tris-HCl, pH 7.0) and were physically disrupted either through three cycles of freezing and thawing or using Ultrasonic Cell Disrupter (BR-2006A, Cosmo Bio, Carlsbad, CA, USA) to release the recombinant virus. The supernatants were collected after centrifuging two or three times at 4,000 rpm for 10 min at 4°C. The supernatant containing the virus was loaded slowly over a 36% sucrose solution and centrifuged at 13,700 rpm for 80 min at 4°C. After removing the supernatant completely, the virus pellet was resuspended in a buffer containing 10 mM Tris-HCl, pH 9.0, or 30 mM Tris-HCl, pH 7.7, with 10% sucrose. To determine the titers of the viruses, a TCID₅₀ assay was performed as described in Shin et al., 2020. Briefly, Vero cells were seeded into 96-well plates and infected with the virus at 10-fold serial dilutions in a 2% FBS-containing medium. The cytopathic effects were examined at 4 days post infection using an optical microscope.

Western blotting

HeLa cells in 100-mm cell culture dishes were infected with KLS-3010 or KLS-3020 at an MOI of 0.05. After 48 h of infection, the medium was changed to a serum-free medium. Supernatants were harvested 24 h after medium exchange and centrifuged at 1,500 rpm for 5 min to remove debris. After centrifugation, the supernatant was transferred into Amicon Ultra-15 Centrifugal Filter Unit (UFC901024, Millipore, Burlington, MA, USA) and centrifuged at 4,000 rpm for 40 min at 4°C to concentrate the secreted proteins. Then 1× protease inhibitor cocktail (11836153001, Sigma-Aldrich, Saint Louis, MO, USA) was added. Protein amounts were quantified using BSA standard (5000206, Bio-Rad, Hercules, CA, USA) and Quick Start Bradford Protein Assay (5000205, Bio-Rad), and equal amounts of protein for each sample were used for western blotting. The proteins were separated through SDS-polyacrylamide gel electrophoresis and transferred to a nitrocellulose membrane (162-0177, Bio-Rad) by the wet transferring method. Transferred membranes were blocked with a 5% blotting-grade blocker (1706404, Bio-Rad) for 1 h. After blocking, specific primary antibodies rabbit anti-hPH-20 (LS-C331909, LsBio, Seattle, WA, USA), rat anti-mIL-12 (MAB4991, R&D systems, Minneapolis, MN, USA), and goat anti-mPD1 (AF1021M, R&D Systems) were added to 5% blotting-grade blocker and incubated overnight at 4°C. Then, the membranes were washed three times with 1× TBST (IBS-BT005, Intrabio, Gyeonggi-do, Korea) and treated with specific secondary antibodies: goat anti-rabbit IgG (H + L) (111-035-003, Jackson ImmunoResearch, West Grove, PA, USA) for PH-20, goat anti-rat IgG (whole molecule)-peroxidase antibody (A9037, Sigma-Aldrich) for mIL-12, and rabbit anti-goat IgG (H + L) (31402, Invitrogen, Waltham, MA, USA) for PD-1 and incubated for 1 h at room

temperature. After incubation, the membranes were washed three times with $1 \times$ TBST and treated with enhanced chemiluminescence (ECL) solutions (RPN2232, GE Healthcare, Chicago, IL, USA). After 5 min of ECL treatment, the detected proteins were confirmed using an Imaging System (ChemiDoc MP, Bio-Rad).

mIL-12 ELISA

Then 3×10^5 HeLa cells were seeded on each well of six-well plate and incubated at 37°C with 5% CO_2 . After 24 h, the medium was replaced with fresh medium containing 2% FBS and cells were infected with KLS-3020 virus at the MOI of 0.00025–0.01. After 24 to 48 h from infection, the medium was harvested and centrifuged at 2,000 rpm for 5 min at 4°C to remove debris. After centrifugation, the supernatant was transferred to an e-tube and stored at -20°C . The expression level of mIL-12 was measured by Mouse IL-12 p70 Quantikine ELISA Kit (M1270, R&D systems, Minneapolis, MN, USA).

In vitro PH-20 activity assay

CT26.WT and B16F10 cells were seeded on a 35-mm six-well plate at the confluence of 3×10^5 per well and incubated at 37°C with 5% CO_2 . After 24 h, the medium was replaced with fresh medium containing 2% FBS and infected with the virus of interest at the MOI of 0.1. After 72 h from infection, the conditioned medium was harvested for the analysis. The conditioned medium or standard recombinant hyaluronidase (90101, FUJIFILM Irvine Scientific, Santa Ana, CA, USA) was mixed with 0.1% recombinant HA (H5388, Sigma) solution at the ratio of 1:1 and incubated in a 37°C water bath for 2 h for enzyme reaction. After the reaction, the reactant was mixed with acidic albumin solution (24 mM sodium acetate [S7899, Sigma], 79 mM acetic acid [695092, Sigma] with 0.1% [w/v] BSA [A3294, Sigma], pH 3.75) at the ratio of 1:5 in a 96-well plate and incubated for 10 min at RT. Then the absorbance at 600 nm was assessed and the activity was calculated based on the standard curve from recombinant hyaluronidase.

Animal experiments

Five-week-old male BALB/c mice and female C57BL/6N mice were purchased from KOATECH (Gyeonggi-do, Korea). Mice were housed in the animal facility at Kolon Life Science (Seoul, Korea). All animal experiments were approved by the Institutional Animal Care and Use Committee (IACUC) of Kolon Life Science (approval numbers KLS IACUC-2018-182, -2019-151, -2020-165, -2020-170, -2021-157-1, -2021-161, -2021-166, and -2022-168).

In vivo tumor models

For syngeneic mouse tumor models, murine cancer cells were subcutaneously implanted on the right flanks of 6-week-old female C57BL/6N mice (5×10^5 B16F10 cells) or 6-week-old male BALB/c mice (1×10^6 CT26.WT cells). Mice were randomized into study groups when the average tumor volume reached about 100 mm^3 (7 days after cell inoculation) and injected with 50 μL of PBS or recombinant vaccinia viruses. Each viral injection dose for the *in vivo* studies was chosen based on the dose that significantly reduced tumor volume in each model. For the bilateral syngeneic model, 6-week-old

male BALB/c mice were injected with CT26.WT cells both to the left and right flank (5×10^5 cells to the right and 5×10^4 cells to the left flank, respectively). Mice were randomized into study groups when the average volume tumor on the right flank reached about 100 mm^3 (7 days after cell inoculation) and 50 μL of PBS or virus was injected into the tumor on the right flank three times every 2 days. As a humane endpoint, the mice were euthanized when individual tumor volumes reached 2000 mm^3 .

In vivo anti-tumor efficacy

For *in vivo* efficacy testing, mice bearing tumor cells ($n = 5$ [CT26.WT] or 6 [B16F10] mice/group) received PBS or virus intratumorally at doses of 1×10^7 TCID₅₀ (CT26.WT) or 1×10^5 TCID₅₀ (B16F10), respectively. Tumor volumes and body weights were measured twice a week until the end of the observation period (30 days after virus injection). Tumor volume (V) was calculated by the formula below:

$$V = \frac{\text{length} \times \text{width}^2}{2}$$

Fluorescence microscopy

To measure the viral spread in the tumor, the EGFP-positive area was examined. After 3 days from virus injection, the mice were anesthetized and perfused whole body with 20 mL of 4% paraformaldehyde (PFA) solution. Then the tumor was harvested, fixed in 4% PFA solution overnight, and embedded in optimal cutting temperature (OCT) compound (4583, Sakura Tissue-Tek, Torrance, CA, USA) for frozen sectioning. The frozen block was entirely sectioned to 10- μm thickness using a cryostat (HM550, Thermo Fisher Scientific, Waltham, MA, USA), washed with PBS, and mounted with fluorescence mounting medium (S3023, DAKO, Glostrup, Denmark). Then the sections were analyzed using a fluorescence microscope (Axio scope A1, Zeiss, Oberkochen, Germany). For quantification of the viral spread, three images were obtained from each mouse ($n = 6$ mice/group) and analyzed using NIS-element basic research (BR) software (Nikon, Tokyo, Japan).

Flow cytometry

For the analysis of immune cell populations, tumor-bearing mice ($n = 6$ mice/group) treated with PBS or recombinant viruses were sacrificed 5 days after virus injection to harvest tumors. The tumors were minced into small fragments and then incubated with a mixture of 0.15 mg/mL DNase type I (D5025-375KU, Sigma-Aldrich) and 1 mg/mL collagenase type IV (C5138-1G, Sigma-Aldrich) in serum-free medium at 37°C for 30 min. Erythrocytes were removed using red blood cell (RBC) lysis buffer (420301, BioLegend, San Diego, CA, USA). The dissociated cells were stained with the antibodies or corresponding isotype antibodies listed in Table S1. Fc block (14-0161-85, Thermo Scientific) and normal mouse serum (24-5544-94, Thermo Scientific) were used to prevent non-specific antibody binding before surface antigen staining and intracellular staining, respectively. Live and dead cells were distinguished by a fixable

viability dye (564406 [BD Bioscience], 65-0865-41, or 65-0864-14 [Thermo Fisher Scientific]) and dead cells were excluded from the analysis. Intracellular staining was performed using the Foxp3/Transcription Factor Staining Buffer Set (00-5523-00, Thermo Scientific) according to the manufacturer's protocol. Immunofluorescence was measured on a FACS Verse and analyzed using FACS Diva software (BD Bioscience).

ELISPOT assay

To measure the splenocytes responding to tumor antigens, IFN- γ ELISPOT (551083, BD Bioscience) was performed following the manufacturer's instruction. Briefly, when average tumor volume reaches about 100 mm³, CT26.WT tumor-bearing mice were intratumorally injected with PBS or KLS-3020 at a dose of 8×10^7 TCID₅₀ three times every other day. Twenty-eight days after the last virus injection, the spleen was harvested and homogenized using a cell scrapper on a 70- μ m cell strainer. The homogenates were washed with complete medium (DMEM with 10% FBS, 1% AA, and 2 mM L-glu) and collected in a single conical tube. After centrifuging at $400 \times g$ for 5 min, the pellets were suspended with RBC lysis buffer and incubation for 1 min at RT. Then the cells were centrifuged at $400 \times g$ for 5 min, suspended with complete medium, and passed through a 70- μ m cell strainer to remove the cell debris. Then the 1×10^5 splenocytes were co-incubated with 3×10^4 CT26.WT cells to activate the splenocytes with CT26.WT-specific immune response. Eighteen hours after the incubation, the cells were colored following the application of biotinylated anti-IFN- γ antibody, streptavidin-HRP, and AEC substrates. The numbers of the spot were counted with an ELISPOT reader (Eli.Scan+, AELVIS).

Statistical analysis

Statistical analyses were carried out using Sigma Plot (version 13). Data are expressed as the mean \pm standard error of the mean (SEM). Statistical significance was determined by one-way analysis of variants (ANOVA) with the Tukey's *post hoc* test for multiple comparisons or Student's *t* tests for comparisons between two groups. The analyses for the tumor volume changes were performed by two-way ANOVA with Tukey's multiple comparison test. If the normality test failed, the Kruskal-Wallis test or Mann-Whitney U test was applied. Log rank test was used to statistically compare the survival data. *p* values <0.05 were considered to be statistically significant.

DATA AND CODE AVAILABILITY

Data are available from the corresponding author upon reasonable request.

SUPPLEMENTAL INFORMATION

Supplemental information can be found online at <https://doi.org/10.1016/j.omto.2023.08.013>.

ACKNOWLEDGMENTS

This work was supported in part by the Global High-Tech Biomedicine Technology Development Program (grant no. HI153518) of the National Research Foundation (NRF) and the Korea Health Industry

Development Institute (KHIDI), funded by the Korean government (MSIT and MOHW).

AUTHOR CONTRIBUTIONS

S.-O.H., J.K., J.S., H.C., H.L., S.L., H.C. and S.K. designed the study. J.K., H.C., S.L., E.L., H.K., H.L., S.L., N.Y., and J.A. conducted the experiments and collected the data. S.-O.H., J.K., J.S., H.C., H.L., and S.L. analyzed the data. S.-O.H., J.K., J.S., H.C., H.L., S.L., and S.K. wrote the manuscript. S.-O.H., J.K., J.S., H.C., and S.K. provided critical review of the manuscript. S.-O.H. and S.K. are responsible for the overall content as guarantors.

DECLARATION OF INTERESTS

S.-O.H., J.K., S.L., J.S., H.C., E.L., H.K., and S.K. are current employees of Kolon Life Science. H.L., S.L., N.Y., J.A., and H.C. are former employees of Kolon Life Science.

REFERENCES

- Mellman, I., Hubbard-Lucey, V.M., Tontonoz, M.J., Kalos, M.D., Chen, D.S., Allison, J.P., Drake, C.G., Levitsky, H., Lonberg, N., van der Burg, S.H., et al. (2016). De-Risking Immunotherapy: Report of a Consensus Workshop of the Cancer Immunotherapy Consortium of the Cancer Research Institute. *Cancer Immunol. Res.* 4, 279–288.
- Garon, E.B. (2015). Current Perspectives in Immunotherapy for Non-Small Cell Lung Cancer. *Semin. Oncol.* 42 (Suppl 2), S11–S18.
- Hodi, F.S., O'Day, S.J., McDermott, D.F., Weber, R.W., Sosman, J.A., Haanen, J.B., Gonzalez, R., Robert, C., Schadendorf, D., Hassel, J.C., et al. (2010). Improved survival with ipilimumab in patients with metastatic melanoma. *N. Engl. J. Med.* 363, 711–723.
- Larkin, J., Hatswell, A.J., Nathan, P., Lebmeier, M., and Lee, D. (2015). The Predicted Impact of Ipilimumab Usage on Survival in Previously Treated Advanced or Metastatic Melanoma in the UK. *PLoS One* 10, e0145524.
- Galluzzi, L., Chan, T.A., Kroemer, G., Wolchok, J.D., and López-Soto, A. (2018). The hallmarks of successful anticancer immunotherapy. *Sci. Transl. Med.* 10, eaat7807.
- Raja, J., Ludwig, J.M., Gettinger, S.N., Schalper, K.A., and Kim, H.S. (2018). Oncolytic virus immunotherapy: future prospects for oncology. *J. Immunother. Cancer* 6, 140.
- Li, Q., Tan, F., Wang, Y., Liu, X., Kong, X., Meng, J., Yang, L., and Cen, S. (2022). The gamble between oncolytic virus therapy and IFN. *Front. Immunol.* 13, 971674.
- Kaufman, H.L., Kohlhapp, F.J., and Zloza, A. (2015). Oncolytic viruses: a new class of immunotherapy drugs. *Nat. Rev. Drug Discov.* 14, 642–662.
- Mondal, M., Guo, J., He, P., and Zhou, D. (2020). Recent advances of oncolytic virus in cancer therapy. *Hum. Vaccin. Immunother.* 16, 2389–2402.
- Shin, J., Hong, S.O., Kim, M., Lee, H., Choi, H., Kim, J., Hong, J., Kang, H., Lee, E., Lee, S., et al. (2021). Generation of a Novel Oncolytic Vaccinia Virus Using the IHD-W Strain. *Hum. Gene Ther.* 32, 517–527.
- Guedan, S., Rojas, J.J., Gros, A., Mercade, E., Cascallo, M., and Alemany, R. (2010). Hyaluronidase expression by an oncolytic adenovirus enhances its intratumoral spread and suppresses tumor growth. *Mol. Ther.* 18, 1275–1283.
- Thompson, C.B., Shepard, H.M., O'Connor, P.M., Kadhim, S., Jiang, P., Osgood, R.J., Bookbinder, L.H., Li, X., Sugarman, B.J., Connor, R.J., et al. (2010). Enzymatic depletion of tumor hyaluronan induces antitumor responses in preclinical animal models. *Mol. Cancer Ther.* 9, 3052–3064.
- Mirlekar, B., and Pylayeva-Gupta, Y. (2021). IL-12 Family Cytokines in Cancer and Immunotherapy. *Cancers (Basel)* 13, 167.
- Daud, A.I., DeConti, R.C., Andrews, S., Urbas, P., Riker, A.I., Sondak, V.K., Munster, P.N., Sullivan, D.M., Ugen, K.E., Messina, J.L., and Heller, R. (2008). Phase I trial of interleukin-12 plasmid electroporation in patients with metastatic melanoma. *J. Clin. Oncol.* 26, 5896–5903.

15. Chiocca, E.A., Yu, J.S., Lukas, R.V., Solomon, I.H., Ligon, K.L., Nakashima, H., Triggs, D.A., Reardon, D.A., Wen, P., Stopa, B.M., et al. (2019). Regulatable interleukin-12 gene therapy in patients with recurrent high-grade glioma: Results of a phase 1 trial. *Sci. Transl. Med.* *11*, eaaw5680.
16. Boussiotis, V.A. (2016). Molecular and Biochemical Aspects of the PD-1 Checkpoint Pathway. *N. Engl. J. Med.* *375*, 1767–1778.
17. Topalian, S.L., Drake, C.G., and Pardoll, D.M. (2015). Immune checkpoint blockade: a common denominator approach to cancer therapy. *Cancer Cell* *27*, 450–461.
18. Nirschl, C.J., and Drake, C.G. (2013). Molecular pathways: coexpression of immune checkpoint molecules: signaling pathways and implications for cancer immunotherapy. *Clin. Cancer Res.* *19*, 4917–4924.
19. Liu, Z., Ravindranathan, R., Kalinski, P., Guo, Z.S., and Bartlett, D.L. (2017). Rational combination of oncolytic vaccinia virus and PD-L1 blockade works synergistically to enhance therapeutic efficacy. *Nat. Commun.* *8*, 14754.
20. Zamarin, D., Ricca, J.M., Sadekova, S., Oseledchik, A., Yu, Y., Blumenschein, W.M., Wong, J., Gigoux, M., Merghoub, T., and Wolchok, J.D. (2018). PD-L1 in tumor microenvironment mediates resistance to oncolytic immunotherapy. *J. Clin. Invest.* *128*, 5184.
21. Wang, G., Kang, X., Chen, K.S., Jehng, T., Jones, L., Chen, J., Huang, X.F., and Chen, S.Y. (2020). An engineered oncolytic virus expressing PD-L1 inhibitors activates tumor neantigen-specific T cell responses. *Nat. Commun.* *11*, 1395.
22. Bommareddy, P.K., Shettigar, M., and Kaufman, H.L. (2018). Integrating oncolytic viruses in combination cancer immunotherapy. *Nat. Rev. Immunol.* *18*, 498–513.
23. Ribas, A., Dummer, R., Puzanov, I., VanderWalde, A., Andtbacka, R.H.I., Michielin, O., Olszanski, A.J., Malvehy, J., Cebon, J., Fernandez, E., et al. (2017). Oncolytic Virotherapy Promotes Intratumoral T Cell Infiltration and Improves Anti-PD-1 Immunotherapy. *Cell* *170*, 1109–1119.e10.
24. Zhang, Y., Zhang, H., Wei, M., Mou, T., Shi, T., Ma, Y., Cai, X., Li, Y., Dong, J., and Wei, J. (2019). Recombinant Adenovirus Expressing a Soluble Fusion Protein PD-1/CD137L Subverts the Suppression of CD8(+) T Cells in HCC. *Mol. Ther.* *27*, 1906–1918.
25. Sioud, M., Westby, P., Olsen, J.K.E., and Mobergslie, A. (2015). Generation of new peptide-Fc fusion proteins that mediate antibody-dependent cellular cytotoxicity against different types of cancer cells. *Mol. Ther. Methods Clin. Dev.* *2*, 15043.
26. Mosely, S.I.S., Prime, J.E., Sainson, R.C.A., Koopmann, J.O., Wang, D.Y.Q., Greenawalt, D.M., Ahdesmaki, M.J., Leyland, R., Mullins, S., Pacelli, L., et al. (2017). Rational Selection of Syngeneic Preclinical Tumor Models for Immunotherapeutic Drug Discovery. *Cancer Immunol. Res.* *5*, 29–41.
27. Vähä-Koskela, M., and Hinkkanen, A. (2014). Tumor Restrictions to Oncolytic Virus. *Biomedicines* *2*, 163–194.
28. Toole, B.P. (2004). Hyaluronan: from extracellular glue to pericellular cue. *Nat. Rev. Cancer* *4*, 528–539.
29. Caon, I., Bartolini, B., Parnigoni, A., Caravà, E., Moretto, P., Viola, M., Karousou, E., Vigetti, D., and Passi, A. (2020). Revisiting the hallmarks of cancer: The role of hyaluronan. *Semin. Cancer Biol.* *62*, 9–19.
30. Tang, Z., Li, C., Kang, B., Gao, G., Li, C., and Zhang, Z. (2017). GEPIA: a web server for cancer and normal gene expression profiling and interactive analyses. *Nucleic Acids Res.* *45*, W98–w102.
31. Kiyokawa, J., Kawamura, Y., Ghouse, S.M., Acar, S., Barçın, E., Martínez-Quintanilla, J., Martuza, R.L., Alemany, R., Rabkin, S.D., Shah, K., and Wakimoto, H. (2021). Modification of Extracellular Matrix Enhances Oncolytic Adenovirus Immunotherapy in Glioblastoma. *Clin. Cancer Res.* *27*, 889–902.
32. Sun, C., Mezzadra, R., and Schumacher, T.N. (2018). Regulation and Function of the PD-L1 Checkpoint. *Immunity* *48*, 434–452.
33. Liu, J., Chen, Z., Li, Y., Zhao, W., Wu, J., and Zhang, Z. (2021). PD-1/PD-L1 Checkpoint Inhibitors in Tumor Immunotherapy. *Front. Pharmacol.* *12*, 731798.
34. Ou, W., Thapa, R.K., Jiang, L., Soe, Z.C., Gautam, M., Chang, J.H., Jeong, J.H., Ku, S.K., Choi, H.G., Yong, C.S., and Kim, J.O. (2018). Regulatory T cell-targeted hybrid nanoparticles combined with immuno-checkpoint blockade for cancer immunotherapy. *J. Control Release* *281*, 84–96.
35. Zuo, S., Wei, M., Xu, T., Kong, L., He, B., Wang, S., Wang, S., Wu, J., Dong, J., and Wei, J. (2021). An engineered oncolytic vaccinia virus encoding a single-chain variable fragment against TIGIT induces effective antitumor immunity and synergizes with PD-1 or LAG-3 blockade. *J. Immunother. Cancer* *9*, e002843.
36. Nakao, S., Arai, Y., Tasaki, M., Yamashita, M., Murakami, R., Kawase, T., Amino, N., Nakatake, M., Kurosaki, H., Mori, M., et al. (2020). Intratumoral expression of IL-7 and IL-12 using an oncolytic virus increases systemic sensitivity to immune checkpoint blockade. *Sci. Transl. Med.* *12*, eaax7992.
37. Zhou, F., Feng, B., Yu, H., Wang, D., Wang, T., Ma, Y., Wang, S., and Li, Y. (2019). Tumor Microenvironment-Activatable Prodrug Vesicles for Nanoenabled Cancer Chemotherapy Combining Immunogenic Cell Death Induction and CD47 Blockade. *Adv. Mater.* *31*, e1805888.
38. Dai, P., Wang, W., Yang, N., Serna-Tamayo, C., Ricca, J.M., Zamarin, D., Shuman, S., Merghoub, T., Wolchok, J.D., and Deng, L. (2017). Intratumoral delivery of inactivated modified vaccinia virus Ankara (IMVA) induces systemic antitumor immunity via STING and Batf3-dependent dendritic cells. *Sci. Immunol.* *2*, eaal1713.
39. Xie, L., Wang, G., Sang, W., Li, J., Zhang, Z., Li, W., Yan, J., Zhao, Q., and Dai, Y. (2021). Phenolic immunogenic cell death nanoinducer for sensitizing tumor to PD-1 checkpoint blockade immunotherapy. *Biomaterials* *269*, 120638.
40. Jiang, Y., and Zhan, H. (2020). Communication between EMT and PD-L1 signaling: New insights into tumor immune evasion. *Cancer Lett.* *468*, 72–81.
41. Vinay, D.S., Ryan, E.P., Pawelec, G., Talib, W.H., Stagg, J., Elkord, E., Lichter, T., Decker, W.K., Whelan, R.L., Kumara, H.M.C.S., et al. (2015). Immune evasion in cancer: Mechanistic basis and therapeutic strategies. *Semin. Cancer Biol.* *35* (Suppl.), S185–s198.
42. Liu, Y.T., and Sun, Z.J. (2021). Turning cold tumors into hot tumors by improving T-cell infiltration. *Theranostics* *11*, 5365–5386.
43. Dmitrieva, N., Yu, L., Viapiano, M., Cripe, T.P., Chiocca, E.A., Glorioso, J.C., and Kaur, B. (2011). Chondroitinase ABC I-mediated enhancement of oncolytic virus spread and antitumor efficacy. *Clin. Cancer Res.* *17*, 1362–1372.
44. Kim, J.H., Lee, Y.S., Kim, H., Huang, J.H., Yoon, A.R., and Yun, C.O. (2006). Relaxin expression from tumor-targeting adenoviruses and its intratumoral spread, apoptosis induction, and efficacy. *J. Natl. Cancer Inst.* *98*, 1482–1493.
45. Caruana, I., Savoldo, B., Hoyos, V., Weber, G., Liu, H., Kim, E.S., Ittmann, M.M., Marchetti, D., and Dotti, G. (2015). Heparanase promotes tumor infiltration and antitumor activity of CAR-redirection T lymphocytes. *Nat. Med.* *21*, 524–529.
46. Zaman, S., Chobrutskiy, B.I., Patel, J.S., Callahan, B.M., Tong, W.L., Mihyu, M.M., and Blanck, G. (2019). MMP7 sensitivity of mutant ECM proteins: An indicator of melanoma survival rates and T-cell infiltration. *Clin. Biochem.* *63*, 85–91.
47. Farrera-Sal, M., Moreno, R., Mato-Berciano, A., Maliandi, M.V., Bazan-Peregrino, M., and Alemany, R. (2021). Hyaluronidase expression within tumors increases virotherapy efficacy and T cell accumulation. *Mol. Ther. Oncolytics* *22*, 27–35.
48. Kuriyama, N., Kuriyama, H., Julin, C.M., Lamborn, K., and Israel, M.A. (2000). Pretreatment with protease is a useful experimental strategy for enhancing adenovirus-mediated cancer gene therapy. *Hum. Gene Ther.* *11*, 2219–2230.
49. Nguyen, K.G., Vrabel, M.R., Mantooth, S.M., Hopkins, J.J., Wagner, E.S., Gabaldon, T.A., and Zaharoff, D.A. (2020). Localized Interleukin-12 for Cancer Immunotherapy. *Front. Immunol.* *11*, 575597.
50. Etxeberria, I., Bolaños, E., Quetglas, J.I., Gros, A., Villanueva, A., Palomero, J., Sánchez-Paulete, A.R., Piulats, J.M., Matias-Guiu, X., Olivera, I., et al. (2019). Intratumor Adoptive Transfer of IL-12 mRNA Transiently Engineered Antitumor CD8(+) T Cells. *Cancer Cell* *36*, 613–629.e7.
51. Ahn, H.H., Carrington, C., Hu, Y., Liu, H.W., Ng, C., Nam, H., Park, A., Stace, C., West, W., Mao, H.Q., et al. (2021). Nanoparticle-mediated tumor cell expression of mIL-12 via systemic gene delivery treats syngeneic models of murine lung cancers. *Sci. Rep.* *11*, 9733.
52. Filippone, A., Lanza, M., Mannino, D., Raciti, G., Colarossi, C., Sciacca, D., Cuzzocrea, S., and Paterniti, I. (2022). PD1/PD-L1 immune checkpoint as a potential target for preventing brain tumor progression. *Cancer Immunol. Immunother.* *71*, 2067–2075.
53. Tumeq, P.C., Harview, C.L., Yearley, J.H., Shintaku, I.P., Taylor, E.J.M., Robert, L., Chmielowski, B., Spasic, M., Henry, G., Ciobanu, V., et al. (2014). PD-1 blockade induces responses by inhibiting adaptive immune resistance. *Nature* *515*, 568–571.

54. Xing, X., Guo, J., Ding, G., Li, B., Dong, B., Feng, Q., Li, S., Zhang, J., Ying, X., Cheng, X., et al. (2018). Analysis of PD1, PDL1, PDL2 expression and T cells infiltration in 1014 gastric cancer patients. *Oncoimmunology* 7, e1356144.
55. Droeser, R.A., Hirt, C., Viehl, C.T., Frey, D.M., Nebiker, C., Huber, X., Zlobec, I., Eppenberger-Castori, S., Tzankov, A., Rosso, R., et al. (2013). Clinical impact of programmed cell death ligand 1 expression in colorectal cancer. *Eur. J. Cancer* 49, 2233–2242.
56. Ohigashi, Y., Sho, M., Yamada, Y., Tsurui, Y., Hamada, K., Ikeda, N., Mizuno, T., Yoriki, R., Kashizuka, H., Yane, K., et al. (2005). Clinical significance of programmed death-1 ligand-1 and programmed death-1 ligand-2 expression in human esophageal cancer. *Clin. Cancer Res.* 11, 2947–2953.
57. Sabatier, R., Finetti, P., Mamessier, E., Adelaide, J., Chaffanet, M., Ali, H.R., Viens, P., Caldas, C., Birnbaum, D., and Bertucci, F. (2015). Prognostic and predictive value of PDL1 expression in breast cancer. *Oncotarget* 6, 5449–5464.
58. Dong, Y., Sun, Q., and Zhang, X. (2017). PD-1 and its ligands are important immune checkpoints in cancer. *Oncotarget* 8, 2171–2186.
59. Ding, X.C., Wang, L.L., Zhang, X.D., Xu, J.L., Li, P.F., Liang, H., Zhang, X.B., Xie, L., Zhou, Z.H., Yang, J., et al. (2021). The relationship between expression of PD-L1 and HIF-1 α in glioma cells under hypoxia. *J. Hematol. Oncol.* 14, 92.
60. Hensel, J.A., Khattar, V., Ashton, R., and Ponnazhagan, S. (2019). Characterization of immune cell subtypes in three commonly used mouse strains reveals gender and strain-specific variations. *Lab. Invest.* 99, 93–106.
61. Baird, J.R., Byrne, K.T., Lizotte, P.H., Toraya-Brown, S., Scarlett, U.K., Alexander, M.P., Sheen, M.R., Fox, B.A., Bzik, D.J., Bosenberg, M., et al. (2013). Immune-mediated regression of established B16F10 melanoma by intratumoral injection of attenuated *Toxoplasma gondii* protects against rechallenge. *J. Immunol.* 190, 469–478.
62. Wang, J., Saffold, S., Cao, X., Krauss, J., and Chen, W. (1998). Eliciting T cell immunity against poorly immunogenic tumors by immunization with dendritic cell-tumor fusion vaccines. *J. Immunol.* 161, 5516–5524.
63. Zuo, S., Wei, M., He, B., Chen, A., Wang, S., Kong, L., Zhang, Y., Meng, G., Xu, T., Wu, J., et al. (2021). Enhanced antitumor efficacy of a novel oncolytic vaccinia virus encoding a fully monoclonal antibody against T-cell immunoglobulin and ITIM domain (TIGIT). *EBioMedicine* 64, 103240.
64. Formenti, S.C., and Demaria, S. (2013). Combining radiotherapy and cancer immunotherapy: a paradigm shift. *J. Natl. Cancer Inst.* 105, 256–265.
65. Postow, M.A., Callahan, M.K., Barker, C.A., Yamada, Y., Yuan, J., Kitano, S., Mu, Z., Rasalan, T., Adamow, M., Ritter, E., et al. (2012). Immunologic correlates of the abscopal effect in a patient with melanoma. *N. Engl. J. Med.* 366, 925–931.
66. Havunen, R., Santos, J.M., Sorsa, S., Rantapero, T., Lumen, D., Siurala, M., Airaksinen, A.J., Cervera-Carrascon, V., Tähtinen, S., Kanerva, A., and Hemminki, A. (2018). Abscopal Effect in Non-injected Tumors Achieved with Cytokine-Armed Oncolytic Adenovirus. *Mol. Ther. Oncolytics* 11, 109–121.